



Originally published as:

Staszek, M., Orlecka-Sikora, B., Leptokaropoulos, K., Kwiatek, G., Martinez Garzon, P. (2017): Temporal static stress drop variations due to injection activity at The Geysers geothermal field, California. - *Geophysical Research Letters*, 44, 14, pp. 7168—7176.

DOI: <http://doi.org/10.1002/2017GL073929>



RESEARCH LETTER

10.1002/2017GL073929

Key Points:

- We examined significance of temporal static stress drop changes in relation to injection rate variations at The Geysers geothermal field
- Variations of static stress drop in time are statistically significant
- Changes of static stress drop are inversely related to injection rate fluctuations

Supporting Information:

- Supporting Information S1

Correspondence to:

M. Staszek,
mstaszek@igf.edu.pl

Citation:

Staszek, M., B. Orlecka-Sikora, K. Leptokaropoulos, G. Kwiatek, and P. Martínez-Garzón (2017), Temporal static stress drop variations due to injection activity at The Geysers geothermal field, California, *Geophys. Res. Lett.*, *44*, 7168–7176, doi:10.1002/2017GL073929.





Received 21 APR 2017

Accepted 5 JUL 2017

Accepted article online 6 JUL 2017

Published online 22 JUL 2017

Temporal static stress drop variations due to injection activity at The Geysers geothermal field, California

M. Staszek¹ , B. Orlecka-Sikora¹, K. Leptokaropoulos¹ , G. Kwiatek² , and P. Martínez-Garzón² 

¹Institute of Geophysics, Polish Academy of Sciences, Warsaw, Poland, ²Section 4.2: Geomechanics and Rheology, Helmholtz-Centre Potsdam, GFZ German Research Centre for Geosciences, Potsdam, Germany

Abstract We use a high-quality data set from the NW part of The Geysers geothermal field to determine statistical significance of temporal static stress drop variations and their relation to injection rate changes. We use a group of 322 seismic events which occurred in the proximity of Prati-9 and Prati-29 injection wells to examine the influence of parameters such as moment magnitude, focal mechanism, hypocentral depth, and normalized hypocentral distances from open-hole sections of injection wells on static stress drop changes. Our results indicate that (1) static stress drop variations in time are statistically significant, (2) statistically significant static stress drop changes are inversely related to injection rate fluctuations. Therefore, it is highly expected that static stress drop of seismic events is influenced by pore pressure in underground fluid injection conditions and depends on the effective normal stress and strength of the medium.

1. Introduction

The physical mechanisms which lead to the occurrence of induced seismicity (IS) in fluid injection environments are related to an increase of pore pressure, which causes (1) a decrease of effective normal stress on the fault that diminishes the fault strength and leads to the failure (shear failure) [Ellsworth, 2013] or (2) an opening of new cracks in the rock (tensile openings) [Fischer and Guest, 2011]. Specifically, in the case of geothermal environments thermoelastic stresses, which emerge from the temperature gradient between hot rock and cool injected water, lead to thermal fracturing of rocks and occurrence of IS, especially near the injection well [Martínez-Garzón et al., 2014].

Usually, mentioned mechanisms are well reflected in spatiotemporal distribution of seismicity cloud in relation to injection activity [e.g., Martínez-Garzón et al., 2014; Fang et al., 2016; Goebel et al., 2016; Johnson et al., 2016; Leptokaropoulos et al., 2016]. Moreover, some authors suggested that static stress drop could be influenced by the fluid injection process [Goertz-Allmann et al., 2011; Lengliné et al., 2014]. In this study we refer to the latter statement by analyzing the relation between static stress drop and injection rate with consideration of statistical significance of both parameters' changes. We expect to observe the influence of injection rate on static stress drop values due to its direct impact on pore pressure, and therefore effective normal stress, in the reservoir.

By definition static stress drop ($\Delta\sigma$) is the difference between average shear stress on the fault before and after the earthquake [Kato, 2012; Cocco et al., 2016], and its approximation can be estimated from seismic data. It is observed that $\Delta\sigma$ values range from 0.1 to 100 MPa, and they are generally independent of the seismic moment [e.g., Kanamori and Anderson, 1975; McGarr, 1984; Abercrombie, 1995; Kwiatek et al., 2011] over a wide range of moment magnitudes $-8 < M_w < 9$ [Cocco et al., 2016]. Many factors have been considered as the ones influencing $\Delta\sigma$ values. Some authors suggest that $\Delta\sigma$ depends on hypocentral depth [e.g., Tomic et al., 2009; Baltay et al., 2011; Satoh and Okazaki, 2016], earthquake focal mechanism [Allmann and Shearer, 2009; Kwiatek et al., 2015], or location of seismic event with respect to the tectonic environment (i.e., interplate and intraplate events) [Kanamori and Anderson, 1975; Martínez-Garzón et al., 2015]. Moreover, Feignier and Grasso [1991] and Kwiatek et al. [2011] suggested that rock strength and its level of damage influence $\Delta\sigma$ as well.

It is not easy to assess the variability of $\Delta\sigma$ due to the fact that according to the calculation formula $\Delta\sigma$ values are very sensitive to the uncertainties in estimated corner frequencies [Abercrombie, 2015; Garcia-Aristazabal et al., 2016]. Therefore, it is important to quantify the significance of the results derived from the stress drop analysis.

In this study we analyze statistical significance of temporal changes in the static stress drop of induced seismic events in relation to water injection performed in two wells located in the NW The Geysers geothermal field. Moreover, we examine the influence of other possible factors on the observed significant static stress drop variations. Performed analysis is complemented by the examination of the influence of $\Delta\sigma$ estimation uncertainties on obtained results.

2. Data

The following analysis was performed using a high-quality IS data set from the NW part of The Geysers geothermal field. The cluster of seismicity located in the vicinity of Prati-9 and Prati-29 injection wells consisted of 1254 relocated events [Kwiatek *et al.*, 2015; Martínez-Garzón *et al.*, 2014, 2016, 2017] recorded between 10 of December 2007 and 23 of August 2014 by a local seismic network composed of 31 three-component short-period surface geophones operated by Lawrence-Berkeley National Laboratory. For a representative group of 354 events high-quality stress drops were calculated using mesh spectral ratio technique [Kwiatek *et al.*, 2015]. The technique suppresses the influence of poorly known propagation, site, and sensor effects on source parameters of events forming a cluster. The details of the method are shown in the supporting information Text S1 (see also Kwiatek *et al.* [2011, 2014, 2015] and Harrington *et al.* [2015] for applications of the method in different environments). Moment magnitudes of the events were calculated using the formula of Hanks and Kanamori [1979]. Focal mechanisms were recalculated using a HASH software [Hardebeck and Shearer, 2002] assuming double-couple shear source [Kwiatek *et al.*, 2015].

For the analyses performed within this study a group of 322 events which occurred below the depth of 2.08 km in the time period from 1 February 2010 to 7 August 2014 was used (Figure 1). Twenty six events which occurred at shallower depths were excluded from the analysis in order to eliminate all possible origins of hydrological condition differences between hypocenter locations. Hypocenters of excluded events are located above the open-hole section of Prati-9 (depth of ~ 1.9 km), so the primary factor potentially influencing seismicity is injection into Prati-29, whereas all other events remain under the direct influence of both Prati-9 and Prati-29 injection wells. Moreover, we excluded from the analysis six events which occurred before 1 February 2010 due to the seismic network reconstruction and its potential influence on calculated stress drop values.

Seismicity in this region is associated with injection activity in Prati-9 and Prati-29 wells. Prati-9 well was operating constantly from November 2007 to August 2014, whereas Prati-29 worked from April 2010 to June 2013 [Kwiatek *et al.*, 2015]. Seasonal tendency of injection rates can be observed with peak injection rates occurring during winter months [Martínez-Garzón *et al.*, 2013, 2014; Kwiatek *et al.*, 2015]. Two production wells Prati-4 and Prati-5, where production started in January 2012, are localized east of the analyzed area (Figure 1) [Kwiatek *et al.*, 2015]. In the third nearby production well Prati-25 the production started circa 10 of December 2011 [García *et al.*, 2012]. It has been shown that a clear correlation between seismic activity and injection operations in this area is observable [Martínez-Garzón *et al.*, 2013, 2014; Leptokaropoulos *et al.*, 2016]. Production activity has been proven not to influence seismic activity [Kwiatek *et al.*, 2015]; however, it cannot be neglected in the analysis of temporal static stress drop changes due to its potential impact on pore pressure state.

3. Method

In order to investigate whether the influence of fluid injection process on static stress drop of induced events can be observed in the NW part of The Geysers, we performed Spearman correlation analysis between injection rate values and decimal logarithm of static stress drop (Pa) ($\log(\Delta\sigma)$) averaged over $n = 11-79$ events using moving average method (Figure S1 in the supporting information). The mean value in each $\log(\Delta\sigma)$ averaging window was assigned to the time of first sample in the window. Correlation analysis was performed for injection rates' values from time range 1 February 2010 to 28 April 2012 (Figure 2b); however, $\log(\Delta\sigma)$ of n subsequent events were taken into account due to asymmetric averaging window. The significance of correlation coefficient was determined at 5% significance level.

In the second step of analysis we examined statistical significance of temporal changes of static stress drop. Analysis was performed by comparing medians and distributions of $\log(\Delta\sigma)$ between pairs of nonoverlapping

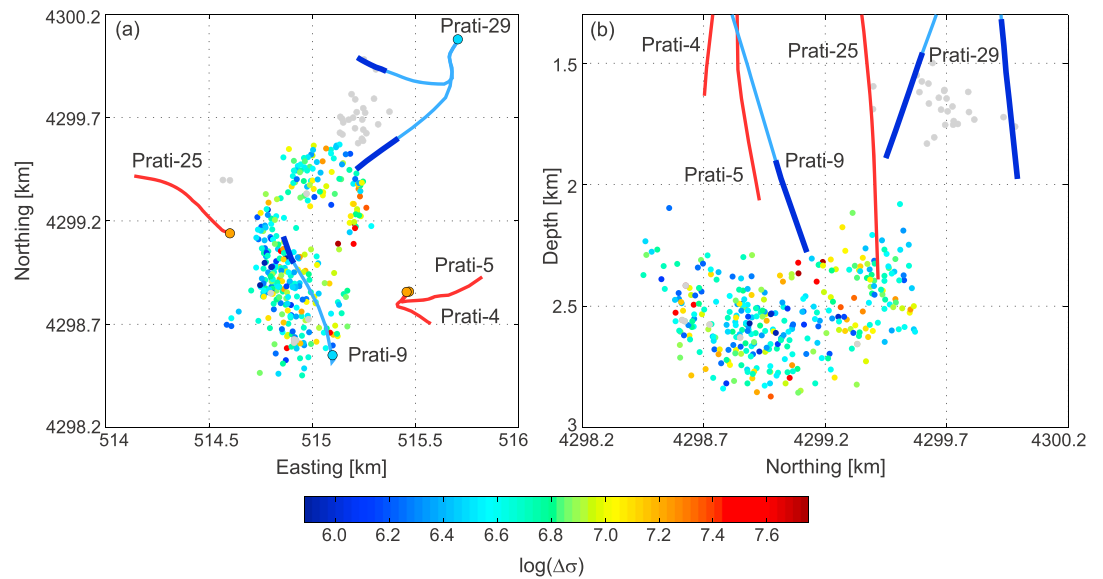


Figure 1. Spatial distribution of 322 seismic events used for the analysis in (a) XY and (b) YZ sections. Decimal logarithms of $\Delta\sigma$ of events are marked as colored dots. Thirty-two events discarded from the analysis are marked as gray dots. Injection wells (Prati-9 and Prati-29) are plotted in blue, whereas production wells (Prati-25, Prati-4, and Prati-5) are marked with red. Open-hole sections of injection wells are marked with dark blue and thickened. The surface end of each well in Figure 1a is assigned with orange (production well) or blue (injection well) circle.

constant Event Windows (EWs) of 20–70 earthquakes shifted by 1 event (Figures 2a and S2 and Table S1). One pair of EWs (EW1 and EW2), which testing result was assigned to event ID = X_0 , included events ($X_0 - EW, X_0 - 1$) and ($X_0 + 1, X_0 + EW$) in EW1 and EW2, respectively, for $X_0 > EW$. For testing $\log(\Delta\sigma)$ median changes nonparametric Wilcoxon rank sum test was used, whereas $\log(\Delta\sigma)$ distribution changes were tested utilizing two-sample Kolmogorov-Smirnov test. The null hypotheses stated that the samples in tested pairs of EWs come from the continuous distributions with equal medians (Wilcoxon test) and that the samples come from the same continuous distributions (Kolmogorov-Smirnov test). Both tests were applied at 5% significance level for null hypotheses rejection. On the basis of obtained results we distinguished three Time Intervals (TIs) with significantly different medians and distributions of $\log(\Delta\sigma)$ (Figure 2b). The procedure of TIs separation is described in detail in the supporting information Text S2.

Finally, we assessed the importance of observed correlation between $\log(\Delta\sigma)$ and injection rates and examined the influence of other factors on observed temporal changes of $\log(\Delta\sigma)$. The factors potentially affecting $\log(\Delta\sigma)$ values in fluid injection environment can be grouped into three categories: (1) parameters describing fluid injection (injection rates into Prati-9 and Prati-29 wells and total injection rate into both wells), (2) source parameters (moment magnitude and focal mechanism), and (3) parameters of spatial distribution of seismicity (hypocentral depth and normalized distances from the open-hole sections of Prati-9 and Prati-29 wells). Injection rates are taken into consideration due to their influence on pore pressure state in the reservoir and therefore strength of the reservoir rocks [Terzaghi, 1923]. Moment magnitude of investigated events is tested to refer to the problem of dependence of static stress drop on scalar seismic moment [Cocco *et al.*, 2016]. Focal mechanism is taken into account due to the observation that strike-slip events analyzed have higher stress drops than normal faulting events [Kwiatek *et al.*, 2015]. Finally, hypocentral depth and normalized hypocentral distances from open-hole sections of injection wells are considered in order to refer to the theory of the dependence of $\Delta\sigma$ on the depth of event [Sato and Okazaki, 2016] and the observation of $\Delta\sigma$ increase with increasing distance from the injection well [Goertz-Allmann *et al.*, 2011; Kwiatek *et al.*, 2014]. Hypocentral distance from the open-hole section of injection well was calculated as hypocentral distance to the nearest point of open-hole section of given injection well. Moreover, each hypocentral distance was normalized toward the distance from the nearest point of the open-hole section to the edge of the ellipsoid enclosing all events, in direction designated by mentioned open-hole section point and given hypocenter. Normalization was undertaken in order to eliminate the effect of anisotropic fluid propagation in the

reservoir, which is reflected by the ellipsoidal shape of seismicity cloud [Martínez-Garzón *et al.*, 2014]. In order to quantify the influence of listed parameters on temporal $\log(\Delta\sigma)$ variations we divided each series into distinguished TIs and tested statistical significance of each parameter median and distribution variations between TIs (Figures 3b–3i) using Wilcoxon and Kolmogorov-Smirnov tests, respectively. Two-sample Kolmogorov-Smirnov test (column 3 in Figure 3) provides information whether there are other reasons than median differences, e.g., variation, skewness, and kurtosis differences, for considering variables' distributions as unequal. For testing the statistical significance of focal mechanism changes between TIs chi-squared test at 5% significance level was used due to the categorical character of the variable.

Moreover, we analyzed temporal changes of $\log(\Delta\sigma)$ in spatial seismicity clusters, distinguished using *k*-means method within the entire seismicity cloud, in order to prove that observed changes of $\log(\Delta\sigma)$ in time are not a result of the occurrence of events in distant parts of reservoir with different geomechanical properties [Martínez-Garzón *et al.*, 2014; Kwiatak *et al.*, 2015]. Detailed information concerning cluster analysis method is available in the supporting information Text S3. Statistical analysis of the influence of static stress drop estimation uncertainties on the significance of its temporal changes is presented in detail in the supporting information Text S4.

4. Results

Spearman correlation analysis revealed that significant negative correlation between total, Prati-9, and Prati-29 injection rates and $\log(\Delta\sigma)$ can be observed in the entire analyzed range of 11–79 event $\log(\Delta\sigma)$ smoothing windows (Figure S1). Generally, the strongest correlation was observed between injection rate into Prati-29 well and $\log(\Delta\sigma)$ and the weakest between Prati-9 injection rate and $\log(\Delta\sigma)$. Depending on the well (Prati-9, Prati-29, or both), maximum absolute values of Spearman correlation coefficients equaled 0.38, 0.52, and 0.43 and were obtained for $\log(\Delta\sigma)$ smoothing event windows of 59, 50, and 49 events, respectively. The $\log(\Delta\sigma)$ smoothing window sizes of 49–59 events, for which maximum correlations were obtained, correspond to the time period of ~ 250–300 days. Therefore, they cannot be treated as a time of reservoir response to injection rate changes. It is rather a result of significant $\log(\Delta\sigma)$ decrease, which was recognized by Wilcoxon and Kolmogorov-Smirnov tests in the range of event IDs ~ 48–60, that corresponds to the time period of June–October 2010 (Figure 2a).

During analyzing the relation between injection process intensity and $\log(\Delta\sigma)$, it is important to determine statistical significance of both parameters' changes. Therefore, we first tested statistical significance of $\log(\Delta\sigma)$ temporal changes (Figures 2 and S2, and Tables S1 and S2) and then checked if changes of injection rates in distinguished TIs are statistically significant (Figures 3b–3d). The results of testing statistical significance of $\log(\Delta\sigma)$ medians' and distributions' variations between pairs of 50-event windows, which is the EW size for which the strongest correlation between injection rate into Prati-29 and averaged $\log(\Delta\sigma)$ was obtained, are presented in Figure 2a. It can be observed that significant changes of $\log(\Delta\sigma)$ medians have been recognized twice: circa September 2010 and circa September 2011 (Figure 2a). First significant $\log(\Delta\sigma)$ median change is accompanied by significant $\log(\Delta\sigma)$ distribution change, but in the case of second $\log(\Delta\sigma)$ median change Kolmogorov-Smirnov test did not establish a significant $\log(\Delta\sigma)$ distribution change. However, the results of testing statistical significance of $\log(\Delta\sigma)$ changes between pairs of 20–70 EWs, described in the supporting information Text S2, indicate that both mentioned significant $\log(\Delta\sigma)$ changes can be observed over wide ranges of EWs by both statistical tests (Figure 2a and Table S1). Moreover, the changes can be treated as reliable due to small influence of stress drop estimation uncertainties on the results (Table S2). Therefore, on the basis of these two significant $\log(\Delta\sigma)$ changes, we distinguished three TIs with significantly different levels of $\log(\Delta\sigma)$: first TI comprises time period from 1 February 2010 to 13 September 2010, second TI includes events from 23 September 2010 to 21 August 2011, and third TI comprises time period from 28 August 2011 to 7 August 2014 (Figure 2b). The mean values and standard errors of $\log(\Delta\sigma)$ in each TI are presented in Figure 2b. It can be observed that mean $\log(\Delta\sigma)$ values are lower in the second TI than in the first and third TIs. Visual evaluation of $\log(\Delta\sigma)$ trend in comparison with total injection rate changes reveals that lower mean $\log(\Delta\sigma)$ values correlate in time with two highest total injection rate peaks (Figure 2b). Moreover, high values of $\log(\Delta\sigma)$ in the third TI coincide in time with the start of production in nearby production wells.

In the next step of the analysis we determined statistical significance of injection rate changes between distinguished TIs. Subsequently, we assessed the importance of observed relation between $\log(\Delta\sigma)$ and

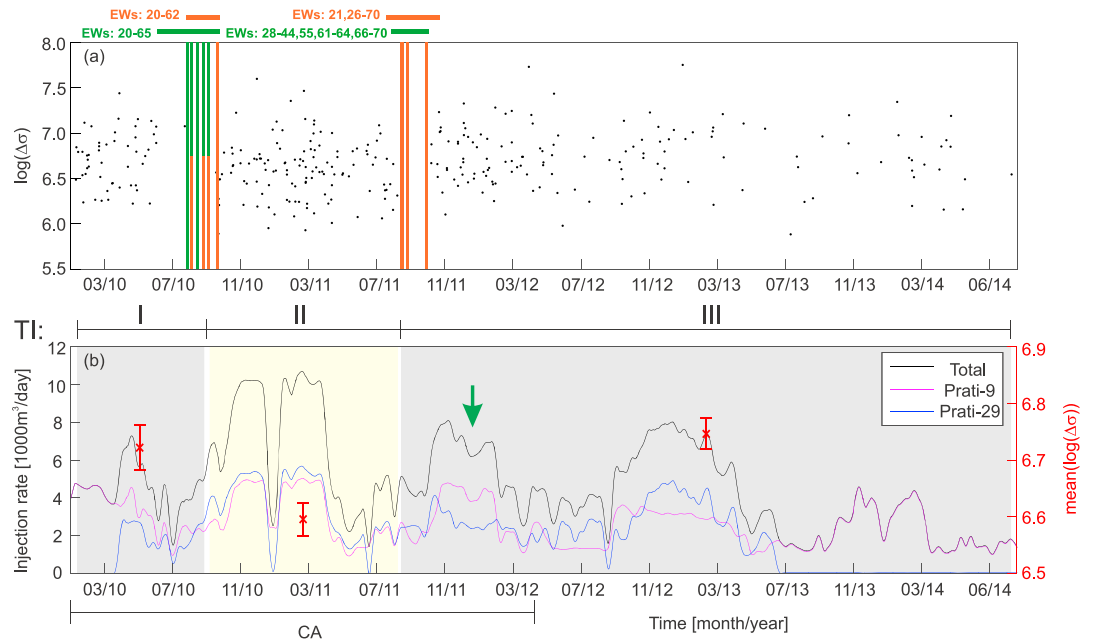


Figure 2. (a) Significant temporal changes of $\log(\Delta\sigma)$ identified in 50-event windows and (b) injection rates variability in distinguished TIs. Black dots in Figure 2a represent $\log(\Delta\sigma)$ values of each event. Orange and green vertical solid lines indicate event IDs (X_0) for which significant $\log(\Delta\sigma)$ changes in 50-event windows were identified by Wilcoxon and Kolmogorov-Smirnov tests, respectively. Solid horizontal lines above Figure 2a indicate ranges of X_0 for which significant $\log(\Delta\sigma)$ changes were identified in 20- to 70-event windows (for details see the supporting information Text S2). Detailed ranges of EWs in which these changes were identified are given on the left side of each line. Color assignment is the same as in the case of vertical lines. In Figure 2b red crosses indicate mean values of $\log(\Delta\sigma)$, and error bars represent standard errors of $\log(\Delta\sigma)$ in each TI. Gray and yellow shaded bars indicate temporal duration of TIs. Green arrow shows the start of production in nearby production wells. The time period from which injection rates' values were used for correlation analysis is assigned as CA.

injection rates in reference to other factors which can affect $\log(\Delta\sigma)$ values in fluid injection environment, such as moment magnitude, focal mechanism, hypocentral depth, and normalized distances from the open-hole sections of Prati-9 and Prati-29 wells. Statistical significance of the aforementioned parameters and their distribution variations is presented in Figures 3b–3h (columns 2–3). In order to better visualize the results, changes of listed parameters are presented schematically in column 4 of Figure 3. We observed statistically significant changes of medians and distributions of total injection rate between adjacent TIs distinguished on the basis of $\log(\Delta\sigma)$ values (Figure 3b). Significant change of the median of injection rate into Prati-9 well is not recognized until third TI when it drops significantly; however, its distributions differ significantly for all combinations of TIs (Figure 3c), as it is in the case of total and Prati-29 injection rates (Figures 3b and 3d). The median values of injection rate observed at Prati-29 well reveal the same statistical behavior as medians of total injection rate (Figure 3d). Moment magnitude appears to have no connection with $\log(\Delta\sigma)$ changes, because Wilcoxon test did not confirm the statistical significance of magnitude changes between considered TIs (Figure 3e). The other parameter which could explain changes of $\Delta\sigma$ in time is hypocentral depth. However, in this case, hypocentral depth of events increases significantly only in the third TI (Figure 3f). For this reason, depth cannot explain the change of $\log(\Delta\sigma)$ between the first and second TIs. What is more, Spearman correlation analysis does not reveal existence of statistically significant correlation between $\log(\Delta\sigma)$ and depth of events (p value equals 0.972). Referring to the observation of Goertz-Allmann *et al.* [2011] and Kwiatek *et al.* [2014], no relation between $\log(\Delta\sigma)$ and normalized distances from both injection wells changes can be identified (Figures 3g and 3h). Finally, chi-squared test did not reveal the existence of statistically significant change in the contents of normal, strike-slip and thrust faulting events between TIs (p value equals 0.675; Figure S5; compare with Figure 3 in Kwiatek *et al.* [2015]). However, this result does not exclude the possibility that such a change does occur, due to the fact that statistical inference is conclusive only in the case of null hypothesis rejection.

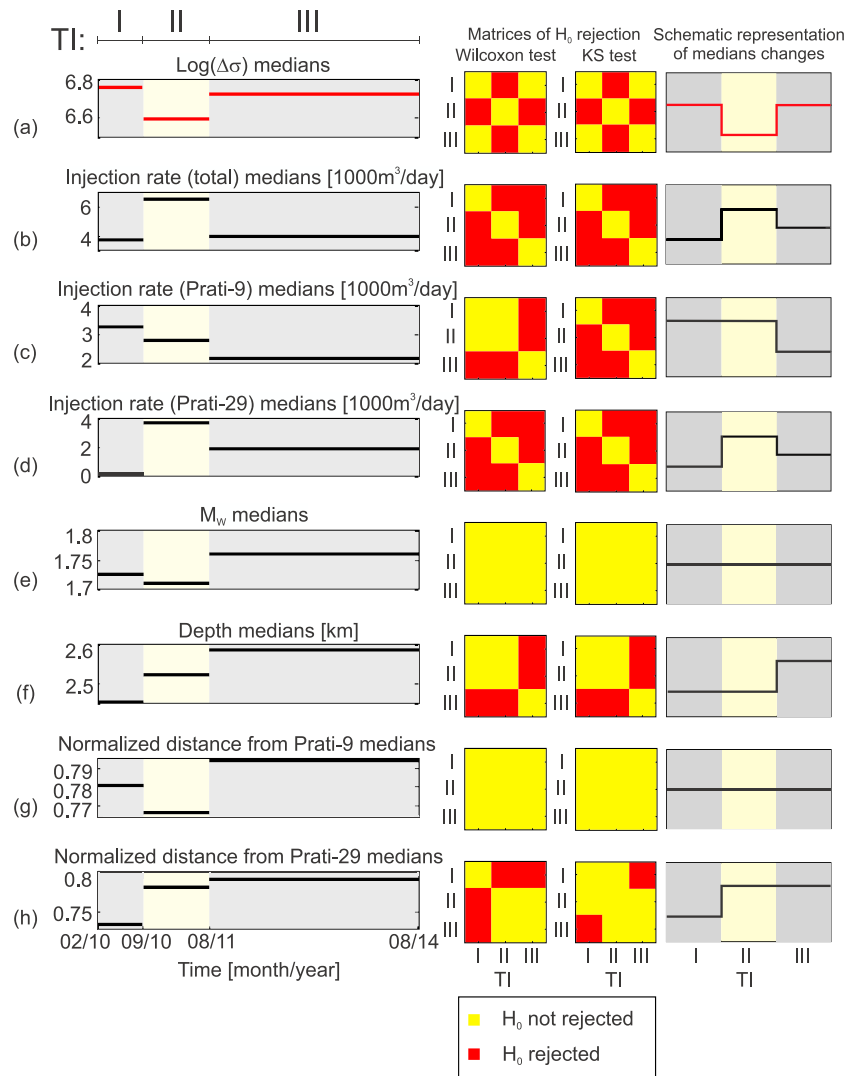


Figure 3. Analysis of the dependence of $\log(\Delta\sigma)$ temporal changes on other parameters' variations. In the first column median values of chosen parameters in three TIs are plotted in time. Second and third columns present the results of testing the statistical significance of parameters' variations using Wilcoxon and two-sample Kolmogorov-Smirnov tests, respectively. The fourth column shows schematic representation of statistically significant temporal changes of chosen parameters.

Other factors that can strongly affect $\Delta\sigma$ values are geomechanical properties and the level of damage of the rocks [Kwiatek et al., 2011]. These parameters are considered here in terms of spatial distribution of the earthquake hypocenters. We assume that events clustered in space occur in areas which have similar rock properties and level of damage. Obtained results, presented in detail in the supporting information Text S3, reveal that in $\sim 94\%$ of cases significant temporal $\log(\Delta\sigma)$ changes occur in at least one cluster among eight distinguished (Table S3). Therefore, we suggest that significant changes of $\log(\Delta\sigma)$ medians and distributions, identified for the entire data set, are not an effect of rheological reservoir differentiation.

Summarizing, the only parameters we can consider here as the ones influencing $\log(\Delta\sigma)$, at least during the first and second TIs, are total injection rate and injection rate into Prati-29. There are two possible explanations for such a result. First, it can be suggested that the decrease of $\log(\Delta\sigma)$ in second TI is a result of the exceedance of some boundary level of total injection rate. The alternative hypothesis states that a delayed reaction of $\log(\Delta\sigma)$ changes to the start of injection into Prati-29 well occurs. However, regardless the agreed scenario, the same physical mechanism explaining obtained results can be proposed.

Significant temporal changes of $\log(\Delta\sigma)$ observed together with significant injection rate changes, and confirmed by the negative correlation between both parameters, suggest that $\log(\Delta\sigma)$ variations in analyzed area can be considered as a consequence of pore pressure and rock strength changes in the reservoir connected with the significant variations of injection rate. An increase of pore pressure during high injection interval leads to the decrease of effective normal stress and rock strength [Terzaghi, 1923] and therefore may cause static stress drop decrease. It is important to note that pore pressure state in the reservoir can be also influenced by the production activity, which starts at the beginning of the third TI (Figure 2b). The quantitative analysis of production activity is out of the scope of this study; however, it is mentioned here as a potential factor responsible for $\log(\Delta\sigma)$ changes.

Finally, it is important to assess the susceptibility of obtained results on $\log(\Delta\sigma)$ estimation uncertainties. The results of such analysis, presented in detail in the supporting information Text S4, reveal that in over 70% of cases the pattern of $\log(\Delta\sigma)$ median changes identified using mean values of $\log(\Delta\sigma)$ is obtained (compare column 2 of Figure 3a and Table S4). The solutions are more scattered in case of $\log(\Delta\sigma)$ distribution changes, where slightly over 50% of cases reveal the $\log(\Delta\sigma)$ mean values pattern (compare column 3 of Figure 3a and Table S4). Therefore, we conclude that both $\log(\Delta\sigma)$ median and distribution changes patterns identified using mean values of $\log(\Delta\sigma)$ are the most probable solutions after considering $\log(\Delta\sigma)$ estimation uncertainties. However, $\log(\Delta\sigma)$ median changes pattern is more resistant to $\log(\Delta\sigma)$ uncertainties than the pattern of $\log(\Delta\sigma)$ distribution changes.

5. Discussion

The observed relation between $\log(\Delta\sigma)$ and injection rate can be explained by the dependence of $\Delta\sigma$ on pore pressure in the reservoir and consequently on the strength of the medium. Such a relation was previously suggested by Goertz-Allmann *et al.* [2011] who observed an increase of static stress drop with the distance from injection well during reservoir stimulation at Deep Heat Mining project in Basel, Switzerland. Similar observation was made by Kwiatak *et al.* [2014] in Berlín geothermal field, El Salvador. In the case of analyzed seismicity cluster no relation between $\Delta\sigma$ and the distance from injection wells has been observed, probably due to the combined seismic effect from Prati-9 and Prati-29 injection wells and potential presence of the local fault in the vicinity of injection area [Martínez-Garzón *et al.*, 2014]. Moreover, in the analyzed area we expect quick fluid propagation and therefore lower pressure buildup in comparison to Basel site, which could also make this effect not observable. However, temporal changes of $\log(\Delta\sigma)$ related to injection (and possibly production) activity suggest that $\Delta\sigma$ values change due to pore pressure changes in the reservoir. This concept is strongly supported by temporal changes in seismic activity correlated with injection activity [Martínez-Garzón *et al.*, 2013; Leptokaropoulos *et al.*, 2016]: more seismic events are registered during time periods of high injection rates which leads to pore pressure increase and consequently reduction of effective normal stress and reservoir strength [Terzaghi, 1923]. Similar concept has been proposed by Lengliné *et al.* [2014] for Soultz-sous-Forêts geothermal reservoir on the basis of observation that events which occurred at the same location may exhibit stress drop variations by a factor of 300. However, they did not observe any trend of $\Delta\sigma$ temporal changes and compare it with injection rate variations. According to Martínez-Garzón *et al.* [2014], maximum pore pressure change (Δp) between peak and preinjection/postinjection periods in analyzed area is ~ 1 MPa, which implies a decrease of critical shear stress on every fault plane by 0.85 MPa during peak injection period assuming friction coefficient is 0.85 [Byerlee, 1978]. Medians of stress drop change from 5.71 to 3.92 MPa between the first and second TIs. This means that $\Delta p = 1$ MPa can explain almost 50% of observed $\Delta\sigma$ variation. The remaining part of $\Delta\sigma$ change can be explained most likely by Δp estimation uncertainty or other physical processes influencing $\Delta\sigma$ values, as discussed below.

It is worth mentioning that laboratory data also shows the existence of relation between effective normal stress and static stress drop. Median values of $\Delta\sigma$ which McLaskey *et al.* [2014] obtained from acoustic emission data introducing two different values of effective normal stress (4 and 6 MPa) to the experiment equaled to 0.06 and 2.47 MPa, respectively, and this difference is significant due to Wilcoxon test (p value equals 1.27×10^{-5}).

Observed temporal $\Delta\sigma$ changes can also be considered as a result of aseismic slip occurrence in the reservoir. Geothermal reservoirs are exceptionally prone to host aseismic slips due to high temperature and low normal stress which favor stable slip [Scholz, 2002]. Such a phenomenon has been proved to occur, i.e., in

Soultz-sous-Forêts geothermal reservoir [Cornet *et al.*, 1997; Bourouis and Bernard, 2007; Cornet, 2016]. Aseismic slip occurs due to rate-strengthening behavior of the fault or fluid pressurization of rate-weakening fault which brings it to the state of conditional stability [Scholz, 1998, 2002]. Therefore, it is possible that during peak injection rate, when pore pressure increases significantly, preexisting faults experience mainly aseismic slip and observed seismicity releases only a portion of total seismic moment. Such an observation was made by Guglielmi *et al.* [2015] during scientific injection into preexisting fault in southeastern France and could explain lower values of estimated static stress drops during this period.

6. Conclusions

On the basis of statistical significance analysis of $\log(\Delta\sigma)$ temporal variations in relation to changes of other parameters such as injection rates, moment magnitude, focal mechanism, hypocentral depth, and normalized distances from injection wells, we state that in the analyzed part of NW The Geysers geothermal field (1) observed variations of $\log(\Delta\sigma)$ medians and distributions in time are statistically significant and (2) significant temporal $\log(\Delta\sigma)$ variations are inversely related to injection rate fluctuations that strongly suggest that they are a result of pore pressure fluctuations. Therefore, it can be suggested that $\Delta\sigma$ depends on the effective normal stress and strength of the medium, in agreement with statements proposed by Goertz-Allmann *et al.* [2011] and Lengliné *et al.* [2014].

Observed significant changes of $\log(\Delta\sigma)$ distributions in time and their dependence on the operational phase imply the possibility to utilize $\log(\Delta\sigma)$ in seismic hazard assessment for NW part of The Geysers area [Staszek *et al.*, 2016].

Acknowledgments

We would like to thank A. McGarr, S. Lasocki, anonymous reviewer, and the Editor for their comments and suggestions that helped improve the manuscript. We acknowledge Calpine Corporation, Northern California Earthquake Data Center (NCEDC), and Lawrence Berkeley National Laboratory for providing technological and seismic data. This work was supported under SHale gas Exploration and Exploitation induced Risks (SHEER) project funded from the European Union's Horizon 2020 Research and Innovation Programme under grant agreement 640896 and within statutory activities 3841/E-41/S/2017 of the Ministry of Science and Higher Education of Poland. M.S. contribution was partially supported by the Ministry of Science and Higher Education of Poland under project 500-10-27. P.M.G. acknowledges funding from the Helmholtz Association in the frame of the Helmholtz Postdoc Programme. Original seismic data are available via NCEDC website <http://ncedc.org/>. The raw injection data and relocated seismic data are available via IS-EPOS platform (<https://tcs.ah-epos.eu>) after registration and providing affiliation.

References

- Abercrombie, R. (1995), Earthquake source scaling relationships from -1 to $5 M_L$ using seismograms recorded at 2.5 km depth, *J. Geophys. Res.*, *100*(B12), 24015–24036, doi:10.1029/95JB02397.
- Abercrombie, R. E. (2015), Investigating uncertainties in empirical Green's function analysis of earthquake source parameters, *J. Geophys. Res. Solid Earth*, *120*, 4263–4277, doi:10.1002/2015JB011984.
- Allmann, B., and P. Shearer (2009), Global variations of stress drop for moderate to large earthquakes, *J. Geophys. Res.*, *114*, B01310, doi:10.1029/2008JB005821.
- Baltay, A., S. Ide, G. Prieto, and G. Beroza (2011), Variability in earthquake stress drop and apparent stress, *Geophys. Res. Lett.*, *38*, L06303, doi:10.1029/2011GL046698.
- Bourouis, S., and B. Bernard (2007), Evidence of coupled seismic and aseismic fault slip during water injection in the geothermal site of Soultz (France), and implication for seismogenic transients, *Geophys. J. Int.*, *169*(2), 723–732, doi:10.1111/j.1365-246X.2006.03325.x.
- Byerlee, J. D. (1978), Friction of rocks, *Pure Appl. Geophys.*, *116*(4–5), 615–626, doi:10.1007/BF00876528.
- Cocco, M., E. Tinti, and A. Cirella (2016), On the scale dependence of earthquake stress drop, *J. Seismol.*, *20*(4), 1151–1170, doi:10.1007/s10950-016-9594-4.
- Cornet, F. H. (2016), Seismic and aseismic motions generated by fluid injections, *Geomech. Energy Environ.*, *5*, 42–54, doi:10.1016/j.gete.2015.12.003.
- Cornet, F. H., J. Helm, H. Poitrenaud, and A. Etchecopar (1997), Seismic and aseismic slips induced by large scale fluid injections, *Pure Appl. Geophys.*, *150*, 563–583, doi:10.1007/978-3-0348-8814-1_12.
- Ellsworth, W. L. (2013), Injection induced earthquakes, *Science*, *341*, doi:10.1126/science.1225942.
- Eshelby, J. D. (1957), The determination of the elastic field of an ellipsoidal inclusion, and related problems, *Proc. R. Soc. London, Ser. A*, *241*(1226), 376–396, doi:10.1098/rspa.1957.0133.
- Fang, Y., S. A. M. den Hartog, D. Elsworth, C. Marone, and T. Cladouhos (2016), Anomalous distribution of microearthquakes in the Newberry geothermal reservoir: Mechanisms and implications, *Geothermics*, *63*, 62–73, doi:10.1016/j.geothermics.2015.04.005.
- Feignier, B., and Grasso, J. R. (1991), Relation between seismic source parameters and mechanical properties of rocks: A case study, *PAGEOPH*, *137*(3), 175–199, doi:10.1007/BF00876987.
- Fischer, T., and A. Guest (2011), Shear and tensile earthquakes caused by fluid injection, *Geophys. Res. Lett.*, *38*, L05307, doi:10.1029/2010GL045447.
- Garcia, J., M. Walters, J. Beall, C. Hartline, A. Pingol, S. Pistone, and M. Wright (2012), Overview of the northwest geysers EGS demonstration project, paper presented at the 37th Workshop on Geothermal Reservoir Engineering, Stanford Univ. Calif.
- Garcia-Aristazabal, A., M. Caciagli and J. Selva (2016), Considering uncertainties in the determination of earthquake source parameters from seismic spectra, *Geophys. J. Int.*, *207*(2), 691–701, doi:10.1093/gji/ggw303.
- Goebel, T. H. W., S. M. Hosseini, F. Cappa, E. Hauksson, J. P. Ampuero, F. Aminzadeh, and J. B. Saleeby (2016), Wastewater disposal and earthquake swarm activity at the southern end of the Central Valley, California, *Geophys. Res. Lett.*, *43*, 1092–1099, doi:10.1002/2015GL066948.
- Goertz-Allmann, B., A. Goertz, and S. Wiemer (2011), Stress drop variations of induced earthquakes at the Basel geothermal site, *Geophys. Res. Lett.*, *38*, L09308, doi:10.1029/2011GL047498.
- Guglielmi, Y., F. Cappa, J. P. Avouac, P. Henry, and D. Elsworth (2015), Seismicity triggered by fluid injections-induced aseismic slip, *Science*, *348*(6240), 1224–1226, doi:10.1126/science.aab0476.
- Hanks, T. C., and H. Kanamori (1979), A moment magnitude scale, *J. Geophys. Res.*, *84*, 2348–2350, doi:10.1029/JB084iB05p02348.
- Hardebeck, J. L., and P. M. Shearer (2002), A new method for determining first-motion focal mechanisms, *Bull. Seismol. Soc. Am.*, *92*, 2264–2276, doi:10.1785/0120010200.
- Hastings, W. K. (1970), Monte Carlo sampling methods using Markov chains and their applications, *Biometrika*, *57*(1), 97–109.

- Harrington, R. M., G. Kwiątek, and S. M. Moran (2015), Self-similar rupture implied by scaling properties of volcanic earthquakes occurring during the 2004-2008 eruption of Mount St. Helens, Washington, *J. Geophys. Res. Solid Earth*, *120*, 4966–4982, doi:10.1002/2014JB011744.
- Johnson, C. W., E. J. Totten, and R. Bürgmann (2016), Depth migration of seasonally induced seismicity at The Geysers geothermal field, *Geophys. Res. Lett.*, *43*, 6196–6204, doi:10.1002/2016GL069546.
- Kanamori, H., and D. L. Anderson (1975), Theoretical basis of some empirical relations in seismology, *Bull. Seismol. Soc. Am.*, *65*, 1073–1095.
- Kagan, Y. Y. (1991), 3-D rotation of double-couple earthquake sources, *Geophys. J. Int.*, *106*, 709–716.
- Kagan, Y. Y. (2007), Simplified algorithms for calculating double-couple rotation, *Geophys. J. Int.*, *171*(1), 411–418.
- Kato, N. (2012), Dependence of earthquake stress drop on critical slip-weakening distance, *J. Geophys. Res.*, *117*, B01301, doi:10.1029/2011JB008359.
- Kwiątek, G., K. Plenkers, G. Dresen, and JAGUARS Research Group (2011), Source parameters of picoseismicity recorded at Mponeng deep gold mine, South Africa: Implications for scaling relations, *Bull. Seismol. Soc. Am.*, *101*, 6, doi:10.1785/0120110094.
- Kwiątek, G., F. Bulut, M. Bohnhoff, and G. Dresen (2014), High-resolution analysis of seismicity induced at Berlin geothermal field, El Salvador, *Geothermics*, *52*, 98–111, doi:10.1016/j.geothermics.2013.09.008.
- Kwiątek, G., P. Martínez-Garzón, G. Dresen, M. Bohnhoff, H. Sone, and C. Hartline (2015), Effects of long-term fluid injection on induced seismicity parameters and maximum magnitude in northwestern part of The Geysers geothermal field, *J. Geophys. Res. Solid Earth*, *120*, 7085–7101, doi:10.1002/2015JB012362.
- Langliné, O., L. Lamourette, L. Vivin, N. Cuenot, and J. Schmittbuhl (2014), Fluid induced earthquakes with variable stress drop, *J. Geophys. Res. Solid Earth*, *119*, 8900–8913, doi:10.1002/2014JB011282.
- Leptokaropoulos K., M. Staszek, S. Lasocki, and G. Kwiątek (2016), Preliminary results for space-time clustering of seismicity and its connection to stimulation processes, in North-Western Geysers Geothermal Field, 35th General Assembly of the European Seismol. Com., Trieste, Italy.
- Lloyd, S. P. (1982), Least squares quantization in PCM, *IEEE Trans. Inf. Theory*, *28*(2), 129–137, doi:10.1109/TIT.1982.1056489.
- Madariaga, R. (1976), Dynamics of an expanding circular fault, *Bull. Seismol. Soc. Am.*, *66*, 639–666.
- Martínez-Garzón, P., M. Bohnhoff, and G. Kwiątek (2013), Stress tensor changes related to fluid injection at The Geysers geothermal field, California, *Geophys. Res. Lett.*, *40*, 2596–2601, doi:10.1002/grl.50438.
- Martínez-Garzón, P., G. Kwiątek, H. Sone, M. Bohnhoff, G. Dresen, and C. Hartline (2014), Spatiotemporal changes, faulting regimes, and source parameters of induced seismicity: A case study from The Geysers geothermal field, *J. Geophys. Res. Solid Earth*, *119*, 8378–8396, doi:10.1002/2014JB011385.
- Martínez-Garzón, P., M. Bohnhoff, Y. Bez-Zion, and G. Dresen (2015), Scaling of maximum observed magnitudes with geometrical and stress properties of strike-slip faults, *Geophys. Res. Lett.*, *42*, 10,230–10,238, doi:10.1002/2015GL066478.
- Martínez-Garzón, P., G. Kwiątek, M. Bohnhoff, and G. Dresen (2016), Impact of fluid injection on fracture reactivation at The Geysers geothermal field, *J. Geophys. Res. Solid Earth*, *121*, 7432–7449, doi:10.1002/2016JB013137.
- Martínez-Garzón, P., G. Kwiątek, M. Bohnhoff, and G. Dresen (2017), Volumetric components in the earthquake source related to fluid injection and stress state, *Geophys. Res. Lett.*, *44*, 800–809, doi:10.1002/2016GL071963.
- McLaskey, G. C., B. D. Kilgore, D. A. Lockner, and N. M. Beeler (2014), Laboratory generated M–6 earthquakes, *Pure Appl. Geophys.*, *171*, 2601, doi:10.1007/s00024-013-0772-9.
- McGarr, A. (1984), Scaling of ground motion parameters, state of stress, and focal depth, *J. Geophys. Res.*, *89*(B8), 6969–6979, doi:10.1029/JB089iB08p06969.
- Metropolis, N., A. Rosenbluth, M. Rosenbluth, A. Teller, and E. Teller (1953), Equation of state calculations by fast computing machines, *J. Chem. Phys.*, *21*, 1087–1092.
- Mosegaard, K., and A. Tarantola (1995), Monte Carlo sampling of solutions to inverse problems, *J. Geophys. Res.*, *100*(B7), 12, 431–12,447, doi:10.1029/94JB03097.
- Sato, T., and A. Okazaki (2016), Relation between stress drops and depths of strong motion generation areas based on previous broadband source models for crustal earthquakes in Japan, in *Earthquakes, Tsunamis and Nuclear Risks, Prediction and Assessment beyond the Fukushima Accident, Part II*, edited by Katsuhiko Kamae, pp. 77–85, Springer, Japan, doi:10.1007/978-4-431-55822-4_6.
- Scholz, C. H. (1998), Earthquakes and friction laws, *Nature*, *391*(6662), 37–42, doi:10.1038/34097.
- Scholz, C. H. (2002), *The Mechanics of Earthquakes and Faulting*, Cambridge Univ. Press, Cambridge.
- Silverman, B. W. (1986), *Density Estimation for Statistics and Data Analysis. Monographs on Statistics and Applied Probability*, Chapman and Hall, London.
- Snoke, J. (1987), Stable determination of (Brune) stress drops, *Bull. Seismol. Soc. Am.*, *77*, 530–538.
- Staszek, M., B. Orlecka-Sikora, and G. Kwiątek (2016), Static stress drop of induced earthquakes in seismic hazard assessment: Preliminary results from The Geysers geothermal site, 35th General Assembly of the European Seismol. Com., Trieste, Italy.
- Terzaghi, K. (1923), Die Berechnung der Durchlässigkeitsziffer des Tones aus dem Verlauf der hydrodynamische Spannungserscheinungen, *Sitzber. Akad. Wiss. Wien, Abt., IIa*, *132*, 125–138.
- Tomic, J., R. E. Abercrombie, and A. F. Do Nascimento (2009), Source parameters and rupture velocity of small $M \leq 2.1$ reservoir induced earthquakes, *Geophys. J. Int.*, *179*, 1013–1023, doi:10.1111/j.1365-246X.2009.04233.x.